Columnar Stacks of Star- and Tadpole-Shaped Polyoxazolines Having Triphenylene Moiety and Their Applications for Synthesis of Wire-Assembled Gold Nanoparticles

Tomoki Ogoshi,* Sachi Hiramitsu, Tada-aki Yamagishi, and Yoshiaki Nakamoto*

Graduate School of Natural Science and Technology, Kanazawa University, Kakuma-machi, Kanazawa 920-1192, Japan

Received January 25, 2009; Revised Manuscript Received March 10, 2009

ABSTRACT: We report on synthesis, association behavior, and application of six-arm star-shaped and tadpole-shaped amphiphilic polyoxazolines from triphenylene initiators. We synthesized two kinds of novel triphenylene initiators: 2,3,6,7,10,11-hexa(6-bromohexyloxy)triphenylene (initiator for star-shaped polyoxazoline) and 2-(6-bromohexyloxy)-3,6,7,10,11-pentahexyloxytriphenylene (initiator for tadpole-shaped polyoxazoline). Ring-opening cationic polymerization of 2-methyl-2-oxazoline from these initiators successfully produced star- and tadpole-shaped polyoxazolines. Both the star- and tadpole-shaped polyoxazolines formed supramolecular associations in aqueous media due to $\pi-\pi$ stacking of hydrophobic triphenylene moiety. Critical micelle concentrations (CMCs) and amounts of $\pi-\pi$ stacking of the star- and tadpole-shaped polyoxazolines in aqueous media were investigated by ^{1}H NMR and fluorescence measurements. From tapping mode atomic force microscopy (TM-AFM) measurements, the star-shaped polyoxazolines formed straight columnar stacks due to $\pi-\pi$ stacking of hydrophobic disklike core of triphenylene moiety and symmetric star-shaped structure. In contrast, crooked nanowires were observed in the tadpole-shaped polyoxazoline. Tadpole shape was asymmetric, and thus ordered $\pi-\pi$ stacking of hydrophobic triphenylene moiety was suppressed. Moreover, by using the columnar stacks of the star-shaped polyoxazoline as a template, we successfully synthesized wire-assembled gold nanoparticles.

Introduction

The construction of supramolecular architectures is currently a subject of great interest in various fields such as chemistry, biology, physics, and material science.[1−13] For the construction of the supramolecular assemblies, using noncovalent physical interactions such as hydrogen bonding,[1−4] host−guest,[5−9] and charge-transfer[10−13] interactions is a useful approach. Among them, noncovalent $\pi-\pi$ stacking between π-conjugated disk-shaped molecules such as triphenylene, coronene, porphyrin, and metallophthalocyanine has attracted tremendous interests because they form one-dimensional columnar stacks.[14−27] The columnar stacks of disk molecules provide efficient anisotropic electron or energy transport channels along the molecular columns and thus open new optoelectronic applications including photoconductive materials, solar cells, and transistors. However, in order to orderly align π-conjugated molecules and build up columnar channels, introduction of chemical and physical techniques is required. Without these techniques, $\pi-\pi$ stacking of π-conjugated disklike molecules is not effective, and thus π-conjugated disklike molecules formed heterogeneous aggregates.[14] As the chemical and physical techniques to obtain highly ordered columnar stacks, liquid crystal,[16] vacuum deposition,[17] and Langmuir−Blodgett film transfer[18] of π-conjugated disklike molecules have been applied. Furthermore, for the purpose of stabilization of the high ordered columnar stacks, oligomers and polymers containing π-conjugated disk-shaped molecules were synthesized.[19−24] Polymers involving π-conjugated disk molecules at side[19,20] and main chain,[21−23] oligomers of π-conjugated disk molecules[24] were reported. Intercalation of electron acceptors into columnar channels of π-conjugated disklike molecules (electron donors) also enhanced stability of the columnar structures.[25−27]

Herein, we report on construction of high ordered columnar stacks of π-conjugated disklike molecules by using hydrophilic−hydrophobic self-assembly in aqueous media. We synthesized new amphiphilic star- and tadpole-shaped polymers containing π-conjugated disklike molecule of triphenylene moiety. Star polymers comprised of triphenylene core and six polyoxazoline arms (Figure 1a). In tadpole-shaped polymer, triphenylene and polyoxazoline moieties were used as head and tail segments, respectively (Figure 1b). Since these star- and tadpole-shaped polyoxazolines combined hydrophobic triphenylene and hydro-

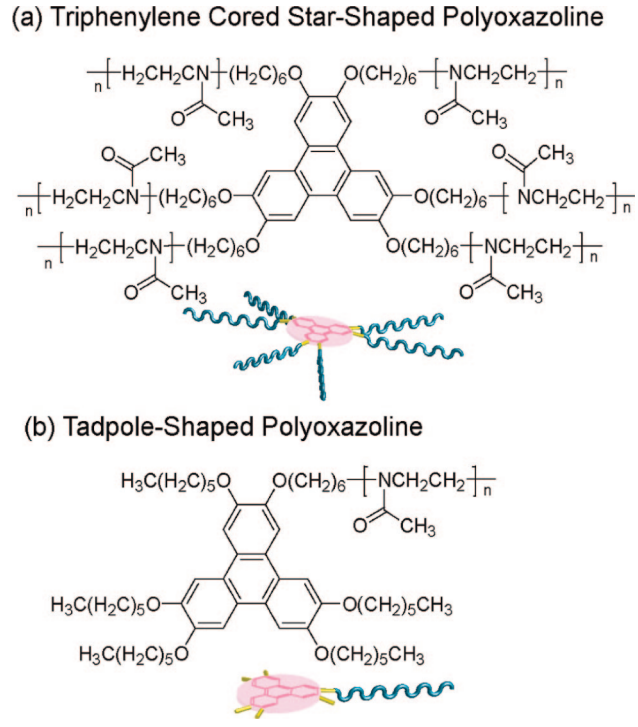

Figure 1. (a) Triphenylene cored star-shaped polyoxazoline and (b) tadpole-shaped polyoxazoline composed of triphenylene head and polyoxazoline tail.

* Corresponding author: Tel +81-76-234-4775; Fax +81-76-234-4800; e-mail ogoshi@t.kanazawa-u.ac.jp.

10.1021/ma900169j CCC: $40.75
Published on Web 03/30/2009

philic polyoxazoline moieties, they formed unique supramolecular columnar associations in aqueous media. In this study, we revealed association property of these amphiphilic polyoxazolines depending on macromolecular shape (star or tadpole) and length of polyoxazoline arms. Investigation on association property depending on the number of polymer arms has been little known. Furthermore, because amide groups of polyoxazoline are able to capture metal ions and work as a protective agent for metal nanoparticles like poly(vinylpyrrolidone),[28,29] we examined synthesis of wire-assembled gold nanoparticles by using the columnar architectures of the star-shaped polyoxazolines as a template.

Experimental Section

Materials. All solvents and reagents were used as supplied except the following. 2-Methyl-2-oxazoline was purchased from Aldrich and distilled from KOH and stored under nitrogen. Anhydrous chloroform was purchased from Kanto Reagents, Chemicals & Biologicals and used for polymerization of 2-methyl-2-oxazoline.

Measurements. The ^{1}H NMR spectra were recorded at 270 MHz, and ^{13}C NMR spectra were recorded at 67.5 MHz with a JEOL-JNM EX270 spectrometer. The FT-IR spectra were obtained using a JASCO FT-IR460 plus infrared spectrometer. Fluorescence spectra were recorded on a Hitachi F-2500 fluorescence spectrometer at room temperature. UV−vis absorption spectra were recorded with a JASCO V-630 and Shimadzu UV-2450 spectrophotometers at room temperature. For fluorescence and UV−vis measurements, 1 cm quartz cuvets were used. The GPC measurements were performed using a Lachrom Elite (Hitachi High-Technologies, Japan) with three columns in series: a TSKguardcolumn Super AW-H and a pair of TSKgelSuper AWM-H (diameter of 6.0 mm; length, 150 mm; and pore size, 9 μm). DMSO containing 10 mmol/L LiBr was used as the eluent (50 °C at 0.5 mL/min). Tapping mode atomic force microscopy (TM-AFM) was taken on multimode SPA 400 (SEIKO Instruments). Nanoprobe cantilevers (SI-DF20, SEIKO Instruments) were utilized. For the preparation of samples, solution of star and tadpole polyoxazolines was deposited on freshly cleaved mica surface and removed the drop by wind pressure immediately.

2,3,6,7,10,11-Hexa-6-(hydroxyhexyloxy)-triphenylene (1) and 2-(6-hydroxyhexyloxy)-3,6,7,10,11-pentahexyloxytriphenylene (2) were prepared according to the literature.[30]

2,3,6,7,10,11-Hexa(6-bromohexyloxy)triphenylene (6BrTP). To a solution of **1** (0.31 g, 0.33 mmol) in THF (3 mL), tetrabromomethane (2.21 g, 6.67 mol) and triphenylphosphine (2.16 g, 8.33 mmol) were added. The mixture was stirred at room temperature for 1 h. The resulting solution was poured into water. The solution was extracted with dichloromethane, and the organic phase was dried over Na_2SO_4 and concentrated. Column chromatography (silica gel, 60% ethyl acetate/40% dichloromethane) afforded a brown semisolid (**6BrTP**, 0.33 g, 0.25 mmol, yield: 76.3%). ^{1}H NMR ($CDCl_3$, 270 MHz, ppm): δ 1.56 (m, 24H, $OCH_2CH_2CH_2CH_2CH_2CH_2$), 1.60 (m, 12H, CH_2CH_2Br), 1.94 (m, 12H, $OCH_2CH_2CH_2$), 3.46 (t, 12H, CH_2Br), 4.23 (t, 12H, OCH_2CH_2), 7.82 (s, 6H, protons from triphenylene moiety). ^{13}C NMR ($CDCl_3$, 67.5 MHz, ppm): δ 25.3 ($OCH_2CH_2CH_2$), 28.0 ($OCH_2CH_2CH_2CH_2$), 29.6 (OCH_2CH_2), 32.7 (CH_2CH_2Br), 33.7 (CH_2Br), 69.6 (OCH_2CH_2), 107.4, 123.8, 149.0 (aromatic carbons from triphenylene moiety). FAB mass m/z = 1303 $(M + H)^+$. Anal. Calcd for $C_{54}H_{78}Br_6O_6$: C, 49.80; H, 6.04; N, 0.00. Found: C, 50.01; H, 5.90; N, 0.00.

2-(6-Bromohexyloxy)-3,6,7,10,11-pentahexyloxytriphenylene (1BrTP). To a solution of **2** (0.21 g, 0.25 mmol) in THF (5 mL), tetrabromomethane (0.55 g, 1.67 mol) and triphenylphosphine (0.55 g, 2.08 mmol) were added. The mixture was stirred at room temperature for 1 h. Then, the mixture was refluxed for 24 h. The resulting solution was poured into water. The solution was extracted with dichloromethane, and the organic phase was dried over Na_2SO_4 and concentrated. Column chromatography (silica gel, 70% dichloromethane/30% hexane) afforded a purple semisolid (**1BrTP**, 0.17 g, 0.19 mmol, yield: 76.0%). ^{1}H NMR ($CDCl_3$, 270 MHz, ppm): δ 0.94 (m, 15H, CH_2CH_3), 1.25, 1.39, 1.56 (m, 36H, $OCH_2CH_2CH_2CH_2CH_2$), 1.94 (m, 12H, $OCH_2CH_2CH_2$), 3.46 (t, 2H, CH_2Br), 4.23 (t, 12H, OCH_2CH_2), 7.83 (s, 6H, protons from triphenylene moiety). ^{13}C NMR ($CDCl_3$, 67.5 MHz, ppm): δ 14.0 (CH_3 from hexyloxy group), 22.6 (CH_2CH_3 from hexyloxy group), 25.3 ($OCH_2CH_2CH_2$ from bromohexyloxy group), 25.7 ($OCH_2CH_2CH_2$ from bromohexyloxy group), 28.0 ($CH_2CH_2CH_2Br$ from bromohexyloxy group), 29.6 (OCH_2CH_2), 31.7 ($CH_2CH_2CH_3$ from hexyloxy group), 32.7 (CH_2CH_2Br from bromohexyloxy group), 33.7 (CH_2Br from bromohexyloxy group), 69.6 (OCH_2CH_2), 107.1, 123.3, 148.7 (aromatic carbons from triphenylene moiety). FAB mass m/z = 906 $(M)^+$. Anal. Calcd for $C_{54}H_{83}BrO_6$: C, 71.42; H, 9.21; N, 0.00. Found: C, 71.63; H, 9.61; N, 0.00.

Scheme 1

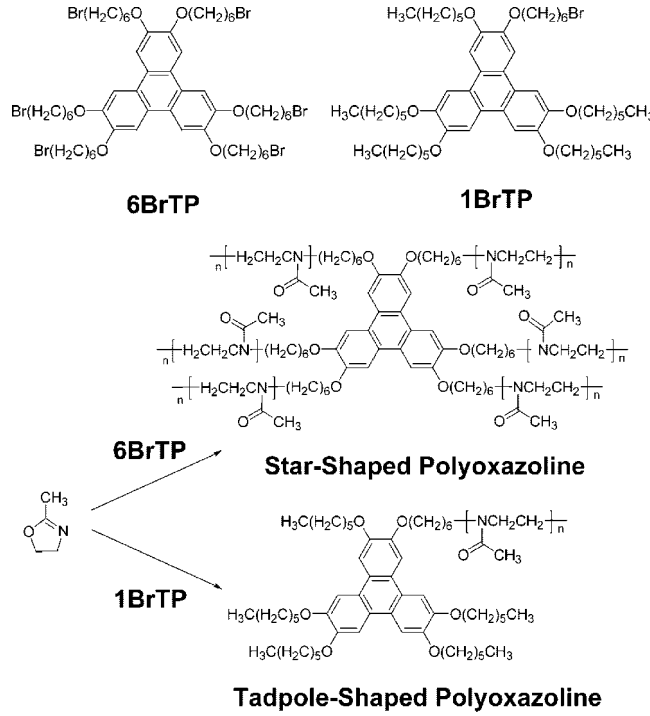

Synthesis of Star- and Tadpole-Shaped Polyoxazolines from Triphenylene Initiators. A typical polymerization procedure is as follows (Scheme 1). To a solution of 2-methyl-2-oxazoline in dehydrated chloroform (5 mL), initiator (**6BrTP** or **1BrTP**) was added at 0 °C under a nitrogen atmosphere. The reaction mixture was refluxed for 72 h. The resulting solution was reprecipitated with diethyl ether repeatedly. After drying in vacuo, star- and tadpole-shaped polyoxazolines were obtained as a slight yellow solid.

Star Polymer. ^{1}H NMR ($CDCl_3$, 270 MHz, ppm): δ 1.56−2.00 (br, 48H, hexyloxy group), 2.00−2.18 (br, methyl group of polyoxazoline), 3.20−.98 (br, 12H, hexyloxy group and ethylene group of polyoxazoline), 4.18−4.28 (br, 12H, hexyloxy group), 7.80−7.84 (br, 6H, protons from triphenylene moiety). ^{13}C NMR ($CDCl_3$, 67.5 MHz, ppm): δ21.2 (carbon from methyl group of polyoxazoline), 21.2, 23.0, 25.3, 27.9, 39.2 (carbons from hexyloxy group), 43.6, 45.2, 46.8, 47.5 (carbons from ethylene group of polyoxazoline), 65.7 (OCH_2CH_2), 107.1, 123.3, 148.5 (aromatic carbons from triphenylene moiety), 170.1 (carbonyl carbon from polyoxazoline). FT-IR (neat, cm^{-1}): 1628 cm^{-1} (the stretching band of amide−carbonyl group), 1258 cm^{-1} (the stretching band of ether group).

Tadpole Polymer. ^{1}H NMR ($CDCl_3$, 270 MHz, ppm): δ 0.85−0.95 (br, 15H, CH_2CH_3), 1.20−2.20 (br, 48H, hexyloxy group), 2.20−2.50 (br, methyl group of polyoxazoline), 3.30−3.95 (br, 2H, hexyloxy group and ethylene group of polyoxazoline), 4.20−4.40 (m, 12H, OCH_2CH_2), 7.82 (s, 6H, protons from

Table 1. Synthesis of Star- and Tadpole-Shaped Polyoxazolines from Triphenylene Initiators

polymer name	initiator	initiator/ monomer	yield (%)	repeating units per arm feed[a]	calcd by ^{1}H NMR	calcd by UV
Star-1	**6BrTP**	1/30	50.2	5	13	16
Star-2	**6BrTP**	1/120	22.1	20	20	26
Star-3	**6BrTP**	1/300	18.4	50	–[b]	54
Star-4	**6BrTP**	1/600	12.5	100	–[b]	46
Tadpole-1	**1BrTP**	1/200	0.37	200	58	60

[a] [Monomer]/number of arms. [b] The peak from triphenylene in polymer was too small to calculate number of repeating units per arm.

triphenylene moiety). FT-IR (neat, cm^{-1}): 1657 cm^{-1} (the stretching band of amide−carbonyl group), 1236 cm^{-1} (the stretching band of ether group).

Synthesis of Gold Nanoparticles in the Presence of Star-Shaped Polyoxazoline as a Template. A typical procedure is described as follows. Star-shaped polyoxazoline was dissolved in aqueous solution. To the solution, $HAuCl_4$ (5.0 mg, 0.012 mmol) was added. Then, aqueous solution of $NaBH_4$ (1.0 mg, 0.027 mmol) was added dropwise for 5 min. The reaction mixture was stirred for 72 h at room temperature. For removal of gold ions from the mixture, dialysis of the solution (cutoff = 3000) was carried out.

Results and Discussion

Synthesis of Star- and Tadpole-Shaped Amphiphilic Polyoxazolines from Triphenylene Initiators. New triphenylene initiators having monobromohexyloxy moiety (**1BrTP**) and hexabromohexyloxy group (**6BrTP**) were synthesized (chemical structures of these initiators are shown in Scheme 1). **1BrTP** and **6BrTP** were characterized by ^{1}H NMR, ^{13}C NMR, FAB-mass, and elemental analysis. By using **6BrTP**, triphenylene cored star-shaped polyoxazolines were prepared. The star-shaped polymers were prepared by varying feed ratio of 2-methyl-2-oxazoline to **6BrTP**. 30, 120, 300, and 600 mol equiv of 2-methyl-2-oxazoline monomer to **6BrTP** were employed (Table 1). The novel six-arm star-shaped polyoxazolines were characterized by ^{1}H NMR, ^{13}C NMR, GPC, UV−vis, and FT-IR measurements. The ^{1}H NMR spectrum of **Star-1** (feed ratios of monomer to initiator are shown in Table 1) is shown in Figure 2b. After polymerization, new proton peaks from polyoxazoline (Figure 2b, peaks d and e) were observed in addition to pristine proton peaks of **6BrTP** (Figure 2a). In addition, the bromomethyl signal of **6BrTP** at 33.7 ppm in the ^{13}C NMR spectrum disappeared after polymerization, strongly suggesting that polymerization of 2-methyl-2-oxazoline occurred from all six-arm of **6BrTP**. From GPC measurements (Supporting Information), a peak derived from **Star-1** was observed at decreased retention time compared to that of **6BrTP**, and the peak showed unimodal distribution. The number of average repeating units of polyoxazoline per arm was determined from the peak integration ratios of methyl protons of polyoxazoline repeating unit at 2.0 ppm to triphenylene protons at 7.8 ppm. In addition, the number of average repeating units was also calculated from UV−vis measurements by using molar absorption coefficient of model compound 2,3,6,7,10,11-hexahexyloxytriphenylene (molar absorption coefficient of 2,3,6,7,10,11-hexahexyloxytriphenylene at wavelength of 347 nm was 3770 M^{-1} cm^{-1}). The data are summarized in Table 1. In **Star-1**, **-2**, and **-3**, the number of average repeating units determined from ^{1}H NMR and UV−vis measurements was increased with increasing of the feed ratio, indicating that the polymerization proceeded clearly. However, in case of **Star-4**, the number of average repeating units determined by UV−vis measurements is smaller than that by the feed. This result can be due to steric hindrance around propagation species along with progress of the polymerization. Furthermore, we synthesized tadpole-shaped polyoxazoline using **1BrTP** as an initiator. The tadpole-shaped

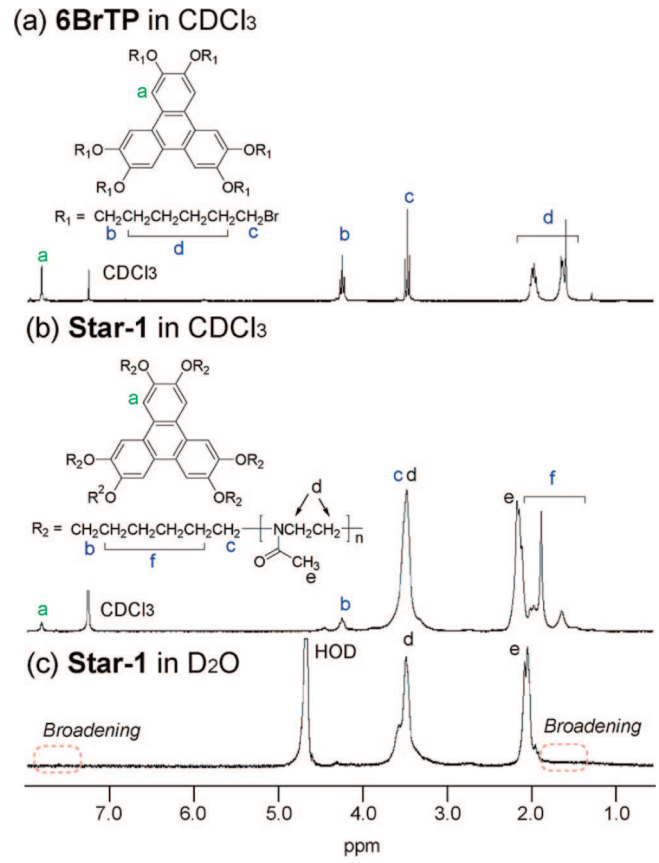

Figure 2. ^{1}H NMR spectra of (a) **6BrTP** in $CDCl_3$, (b) **Star-1** in $CDCl_3$, and (c) **Star-1** in D_2O.

polyoxazoline (**Tadpole-1**) was synthesized by employing 200 mol equiv of 2-methyl-2-oxazoline monomer to **1BrTP**. The chemical structure of **Tadpole-1** was characterized by ^{1}H NMR and FT-IR measurements. As in star-shaped polyoxazolines, **Tadpole-1** exhibited new peaks from polyoxazoline after polymerization, indicating that polymerization of 2-methyl-2-oxazoline took place from **1BrTP** (Supporting Information). The number of average repeating units of polyoxazoline chain was estimated by ^{1}H NMR and UV−vis measurements (Table 1). Even after long reaction times around 72 h, the number of average repeating units of polyoxazoline chain calculated by ^{1}H NMR and UV−vis measurements was shorter than that by the feed. This result is due to the steric hindrance, that is, the decreased initiation activity of the bromohexyloxy group surrounded by bulky triphenylene head. The suppression of the polymerization of 2-methyl-2-oxazoline by bulky initiators was previously reported.[31,32]

Association Behavior of Star- and Tadpole-Shaped Amphiphilic Polyoxazolines in Aqueous Media. The combination of hydrophilic segment of polyoxazoline chain and hydrophobic segment of triphenylene in the star- and tadpole-shaped polymers provides possibilities for unique micellar behavior in aqueous media. Therefore, we revealed the association behavior of the star- and tadpole-shaped polyoxazolines by ^{1}H NMR, fluorescence, and tapping mode atomic force microscopy (TM-AFM) measurements. Figure 2c shows ^{1}H NMR spectrum of the star-shaped polymer (**Star-1**) in D_2O. In D_2O, proton signals of ethylene and methyl groups from polyoxazoline arms were clearly observed, while triphenylene and hexyloxy proton signals were broadening compared to that in $CDCl_3$ (Figure 2b). These data indicate that molecular motion of the hydrophobic triphenylene core and hexyloxy moieties is suppressed due to their transition to the interior of the micelle

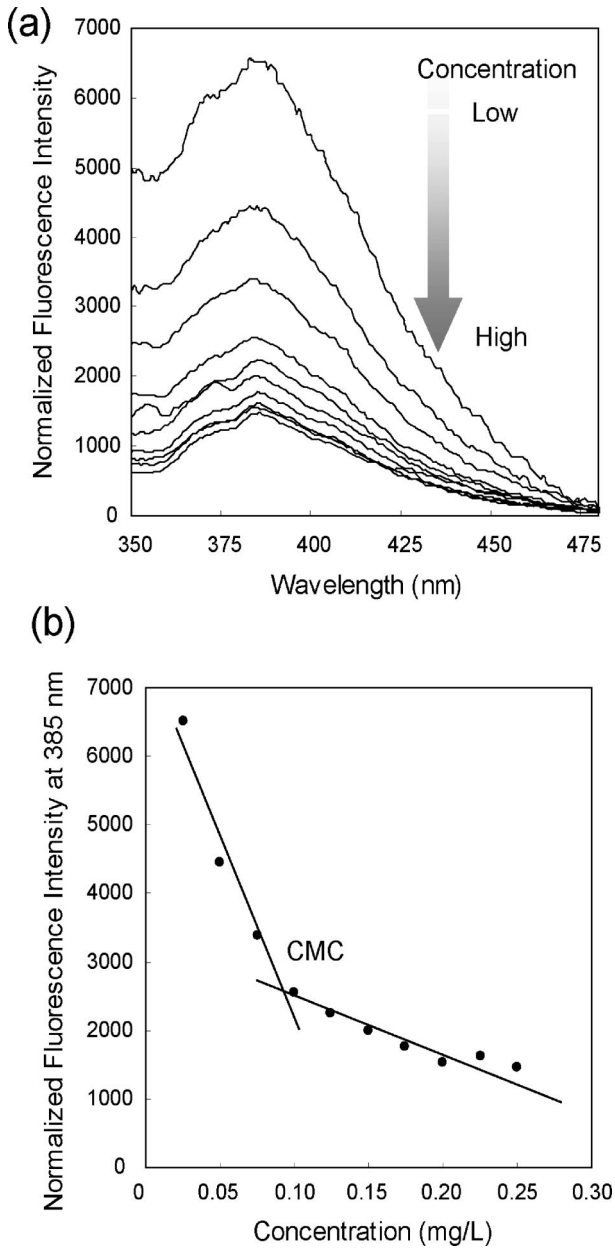

Figure 3. (a) Concentration dependence of the emission spectra of **Star-2** in aqueous media (excited at 280 nm). (b) Fluorescence intensity at 385 nm (normalized by triphenylene concentration) vs concentration of **Star-2**.

in aqueous media. Furthermore, we measured variable temperature ^{1}H NMR of **Star-1** in D_2O (Supporting Information). As the measurement temperature increased, proton resonances from the hexyloxy group around triphenylene core appeared. The data also support the association of hydrophobic hexyloxy group in aqueous media at room temperature. In case of tadpole-shaped polymer (**Tadpole-1**), resonance signals from hexyloxy and triphenylene moieties in D_2O also disappeared, indicating association of hydrophobic hexyloxy and triphenylene segments in aqueous media (Supporting Information). From these observations, both the star- and tadpole-shaped polyoxazolines formed supramolecular assemblies in aqueous media.

The critical micelle concentrations (CMCs) of the star- and tadpole-shaped polyoxazolines in aqueous solutions were determined by a fluorescence technique. We monitored change in fluorescence intensities from triphenylene moiety depending on concentrations of these polyoxazolines. Figure 3a shows emission spectra of **Star-2** depending on concentrations. These peaks

Table 2. Critical Micelle Concentrations of Star- and Tadpole-Shaped Polyoxazolines

	repeating units per arm		
polymer name	calcd by ^{1}H NMR	calcd by UV	CMC (mg/L)
Star-1	13	16	67.0
Star-2	20	26	0.090
Star-3	–[a]	54	670
Star-4	–[a]	46	640
Tadpole-1	58	60	1.58

[a] The peak from triphenylene in polymer was too small to calculate number of repeating units per arm.

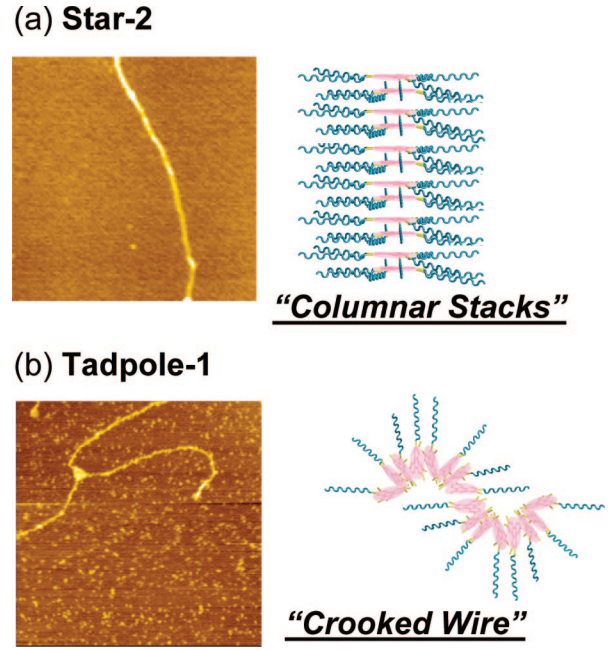

Figure 4. TM-AFM height images of (a) **Star−2** and (b) **Tadpole−1** (1.5 μm × 1.5 μm) from aqueous media.

were normalized by concentrations of triphenylene moiety. In low concentration, emission peak from the triphenylene moiety around 385 nm was strongly observed. However, in high concentration, the emission was quite suppressed. The CMC value was determined from the flexion point of the emission intensity (Figure 3b). The results are summarized in Table 2. **Star-2** showed smallest CMC value among the other star-shaped polyoxazolines. In **Star-2**, hydrophilic polyoxazoline arms should be appropriate length for association of hydrophobic triphenylene cores in aqueous media.

To investigate $\pi-\pi$ stacking of triphenylene segments in the star- and tadpole-shaped polyoxazolines, we measured photoluminescence excitation (PLE) spectra. Relationships between $\pi-\pi$ stacking of triphenylene segments and changes in PLE spectra have been already well-studied.[14] Formation of large amounts of $\pi-\pi$ stacking of triphenylene segments leads to red shifts of PLE spectra. PLE spectra of **Star-2** and **Tadpole-1** in aqueous media were measured at the emission wavelength of 380 nm (Supporting Information). Excitation peak of **Star-1** shifted to longer wavelength compared with that of **Tadpole-1**, indicating that amounts of $\pi-\pi$ stacking of triphenylene moiety in **Star-1** were larger than that in **Tadpole-1**. In the star polyoxazolines, because of their symmetric star structure, $\pi-\pi$ stacking of hydrophobic triphenylene core in aqueous media should easily take place.

Supramolecular architectures from the star- and tadpole-shaped amphiphilic polyoxazolines in aqueous media were investigated by TM-AFM measurements (Figure 4). For the preparation of samples, one drop of the polymer solution was

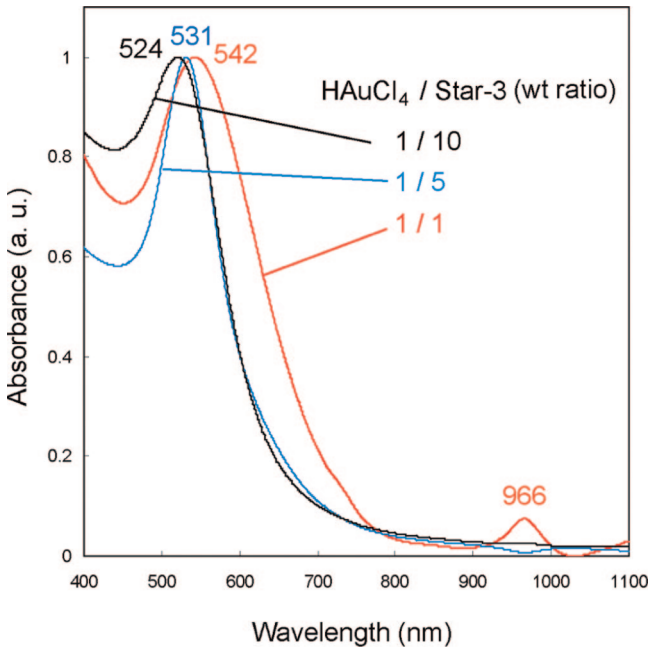

Figure 5. UV−vis spectra of gold nanoparticles protected by **Star−3** in aqueous media. Weight ratios of $HAuCl_4$/**Star−3** are 1/10 (black line), 1/5 (blue line), and 1/1 (red line).

deposited on freshly cleaved mica surface and removed the drop by wind pressure immediately. **Star-2** using chloroform showed heterogeneous spherical aggregates (Supporting Information), indicating that triphenylene core in **Star-2** formed aggregates but was not able to form highly ordered columnar stacks in chloroform. For formation of the ordered columnar stacks, chemical and physical interactions were necessary. The trends were also reported in triphenylene derivatives.[14] On the other hand, in **Star-2** using water, rigid straight columnar stacks were mainly observed (Figure 4a).[33] In this case, planarity of hydrophobic core of triphenylene moiety and symmetric hydrophilic polyoxazoline arms resulted in self-assembly of the rigid columnar stacks in aqueous media. In contrast, **Tadpole-1** partially formed wave wires and free polymers were also observed around the wires (Figure 4b).[33] Since tadpole shape is asymmetric, ordered $\pi-\pi$ stacking of hydrophobic triphenylene head in aqueous media should be difficult. Therefore, **Tadpole-1** formed crooked wires and free polymers were observed. The data supported observations in PLE measurements.

Application of the Star-Shaped Polyoxazolines for Synthesis of Wire-Assembled Gold Nanoparticles. Because amide group of polyoxazoline is able to work as a protecting group for synthesis of metal nanoparticles, we examined formation of gold nanoparticles in the presence of the star-shaped polyoxazoline over CMC concentration. By using **Star-3** as a protecting agent in aqueous media, the solution changed from yellow to red after addition of $NaBH_4$, indicating formation of gold nanoparticles. In contrast, with **Star-3** using methanol as a solvent, precipitation of bulk Au was observed during the reaction. The observations indicate that the columnar assemblies of **Star-3** formed in aqueous media effectively acts as a protecting agent for the synthesis of gold nanoparticles. It is because concentration of polyoxazoline chain should be increased by formation of the columnar associations from **Star-3** in aqueous media. Figure 5 shows UV−vis absorption spectra of the gold nanoparticles with **Star-3** in aqueous media. Surface plasmon adsorption bands around 520−540 nm were observed even in low (red line, $HAuCl_4$/**Star-3** = 1/1), middle (blue line, $HAuCl_4$/**Star-3** = 1/5), and high polyoxazoline (black line, $HAuCl_4$/**Star-3** = 1/10) ratios, indicating the formation of gold nanoparticles in a wide range regardless of $HAuCl_4$/**Star-3** ratios.[34] As the concentrations of **Star-3** decreased, the peak of surface plasmon band was shifted from 524 nm (black line, $HAuCl_4$/**Star-3** = 1/10) to 542 nm (red line, $HAuCl_4$/**Star-3** = 1/1). The trend indicates the formation of the particles aggregates with decreasing of concentrations of protecting agent, **Star-3**.[35] Furthermore, in the sample with the low polyoxazoline ratio (red line, $HAuCl_4$/**Star-3** = 1/1), new peak was observed at 966 nm. The peak should correspond to the longitudinal plasmon bands. It is reported that higher aspect ratio nanoparticles show both transverse and longitudinal plasmon bands.[35−37]

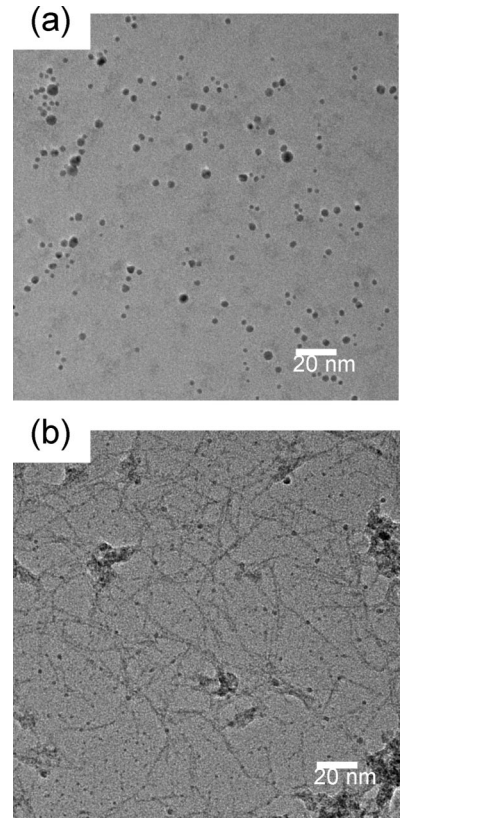

Figure 6. TEM images of gold nanoparticles protected by **Star-3**. Weight ratios of $HAuCl_4$/**Star-3** are 1/10 (a) and 1/1 (b).

Scheme 2

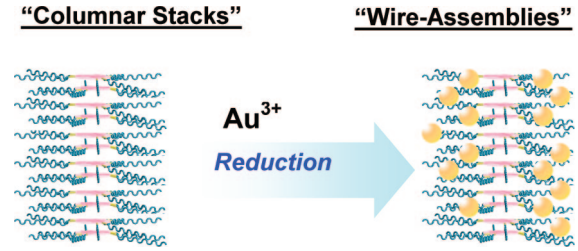

Figure 6 shows TEM images of gold nanoparticles with the high and low polyoxazoline ratios. In the high polyoxazoline ratio (Figure 6a, $HAuCl_4$/**Star-3** = 1/10), sphere-shaped nanoparticles were observed, and the size of the particles was around 2.0 nm. In contrast, in the low polyoxazoline ratio (Figure 6b, $HAuCl_4$/**Star-3** = 1/1), wire-assembled gold nanoparticles were observed. The average diameter and length of the wire-assemblies were 1.0 and 40 nm, respectively. With excessive amounts of protecting agent of **Star-3** ($HAuCl_4$/**Star-3** = 1/10), each gold nanoparticle is dispersed individually. In contrast, with low protecting agent of **Star-3** ($HAuCl_4$/**Star-3** = 1/10), gold nanoparticles assembled along the columnar associations of

Star-3 (Scheme 2). From these observations, it was found that the columnar assemblies of **Star-3** in aqueous media acted as a useful template for synthesis of wire-assembled gold nanoparticles.

Conclusions

We synthesized new star- and tadpole-shaped polyoxazolines using triphenylene initiators. In aqueous media, star- and tadpole-shaped polyoxazolines formed supramolecular associations. From TM-AFM measurements, it was found that star-shaped polyoxazolines formed straight columnar stacks in aqueous media. In contrast, tadpole-shaped polyoxazoline showed crooked nanowires in aqueous solution. Constriction of the wire assemblies covered amphiphilic polyoxazoline chains has been little known. Furthermore, by using the columnar stacks of the star-shaped polyoxazoline as a template, we successfully synthesized wire-assembled gold nanoparticles. Since amphiphilic polyoxazoline is able to capture metal ions and shows superior affinity toward various organic and inorganic materials, the wire assemblies should be applied for catalyst and used as template for construction of tubular organic and inorganic materials.

Acknowledgment. We thank Prof. Kohshin Takahashi (Kanazawa University) for TM-AFM measurements, Mr. Koichi Higashimine (Japan Advanced Institute of Science and Technology) for TEM measurements, and Dr. Jun Araki (Shinshu University) for GPC measurements. A part of this work was conducted in Kyoto-Advanced Nanotechnology Network, supported by "Nanotechnology Network" of the Ministry of Education, Culture, Sports, Science and Technology (MEXT), Japan. This work was supported by a Grant-in-Aid for Young Scientists (WAKATE B-1975011) from MEXT, Japan.

Supporting Information Available: GPC traces of **6BrTP** and **Star-1**, ^{1}H NMR spectra of **Tadpole-1** in $CDCl_3$ and D_2O, variable temperature ^{1}H NMR spectra of **Star-1** in D_2O, photoluminescence excitation spectra of **Star-1** and **Tadpole-1** in aqueous media, TM-AFM height image of **Star-2** prepared from $CHCl_3$, full TM-AFM images of **Star-2** and **Tadpole-1** from water, and XRD pattern of gold nanoparticles stabilized with **Star-3**. This material is available free of charge via the Internet at http://pubs.acs.org.

References and Notes

(1) Brunsveld, L.; Folmer, B. J. B.; Meijer, E. W.; Sijbesma, R. P. *Chem. Rev.* **2001**, *101*, 4071–4098.
(2) Hoeben, F. J. M.; Jonkheijm, P.; Meijer, E. W.; Schenning, A. P. H. J. *Chem. Rev.* **2005**, *105*, 1491–1546.
(3) Roosma, J.; Mes, T.; Leclère, P.; Palmans, A. R. A.; Meijer, E. W. *J. Am. Chem. Soc.* **2008**, *130*, 1120–1121.
(4) Barberá, J.; Puig, L.; Romero, P.; Serrano, J. L.; Sierra, T. *J. Am. Chem. Soc.* **2005**, *127*, 458–464.
(5) Yamauchi, K.; Takashima, Y.; Hashidzume, A.; Yamaguchi, H.; Harada, A. *J. Am. Chem. Soc.* **2008**, *130*, 5024–5025.
(6) Ogoshi, T.; Takashima, Y.; Yamaguchi, H.; Harada, A. *J. Am. Chem. Soc.* **2007**, *129*, 4878–4879.
(7) Kuad, P.; Miyawaki, A.; Takashima, Y.; Yamaguchi, H.; Harada, A. *J. Am. Chem. Soc.* **2007**, *129*, 12630–12631.
(8) Miyauchi, M.; Takashima, Y.; Yamaguchi, H.; Harada, A. *J. Am. Chem. Soc.* **2005**, *127*, 2984–2989.
(9) Ogoshi, T.; Takashima, Y.; Yamaguchi, H.; Harada, A. *Chem. Commun.* **2006**, 3702–3704.
(10) Ghosh, S.; Ramakrishnan, S. *Macromolecules* **2005**, *38*, 676–686.
(11) Ghosh, S.; Ramakrishnan, S. *Angew. Chem., Int. Ed.* **2005**, *44*, 5441–5447.
(12) Ghosh, S.; Ramakrishnan, S. *Angew. Chem., Int. Ed.* **2004**, *43*, 3264–3268.
(13) Gallivan, J. P.; Schuster, G. B. *J. Org. Chem.* **1995**, *60*, 2423–2429.
(14) Duzhko, V.; Shi, H.; Singer, K. D. *Langmuir* **2006**, *22*, 7947–7951.
(15) Kimura, M.; Wada, K.; Ohta, K.; Hanabusa, K.; Shirai, H.; Kobayashi, N. *J. Am. Chem. Soc.* **2001**, *123*, 2438–2439.
(16) Tsukruk, V. V.; Reneker, D. H. *Langmuir* **1993**, *9*, 2141–2144.
(17) Boden, N.; Bushby, R. J.; Martin, P. S. *Langmuir* **1999**, *15*, 3790–3797.
(18) Tsukruk, V. V.; Bengs, H.; Ringsdorf, H. *Langmuir* **1996**, *12*, 754–757.
(19) Weck, M.; Mohr, B.; Maughon, B. R.; Grubbs, G. H. *Macromolecules* **1997**, *30*, 6430–6437.
(20) Cui, L.; Miao, J.; Zhu, L. *Macromolecules* **2006**, *39*, 2536–2545.
(21) Tsukruk, V. V.; Wendorff, J. H. *Langmuir* **1993**, *9*, 614–618.
(22) Huang, C.; Wang, N.; Li, Y.; Li, C.; Li, J.; Liu, H.; Zhu, D. *Macromolecules* **2006**, *39*, 5319–5325.
(23) Kim, Y.; Mayer, M. F.; Zimmerman, S. C. *Angew. Chem., Int. Ed.* **2003**, *42*, 1121–1126.
(24) Cui, L.; Miao, J.; Zhu, L.; Sics, I.; Hsiao, B. S. *Macromolecules* **2005**, *38*, 3386–3394.
(25) Okabe, A.; Fukushima, T.; Ariga, K.; Aida, T. *Angew. Chem., Int. Ed.* **2002**, *41*, 3414–3417.
(26) Markovitsi, D.; Marguet, S.; Bonadkowski, J. *J. Phys. Chem. B* **2001**, *105*, 1299–1306.
(27) Mahlstedt, S.; Janietz, D.; Stracke, A.; Wendorff, J. H. *Chem. Commun.* **2000**, 15–16.
(28) Hirai, H.; Chawanya, H.; Toshima, N. *Bull. Chem. Soc. Jpn.* **1985**, *58*, 682–687.
(29) Toshima, N.; Yonezawa, T. *New J. Chem.* **1998**, *22*, 1179–1201.
(30) Cooke, G.; Radhi, A.; Boden, N.; Bushby, R. J.; Lu, Z.; Brown, S.; Health, S. L. *Tetrahedron* **2000**, *56*, 3385–3390.
(31) Kim, K. M.; Keum, D. K.; Chujo, Y. *Macromolecules* **2003**, *36*, 867–875.
(32) Kim, K. M.; Ouchi, Y.; Chujo, Y. *Polym. Bull.* **2003**, *49*, 341–348.
(33) Full TM-AFM images of the assemblies are shown in the Supporting Information.
(34) Observation of diffraction peaks corresponding to the (111), (200), (220), and (311) planes from X-ray diffraction pattern measurements indicates formation of gold nanoparticles (Supporting Information).
(35) El-Sayed, M. A. *Acc. Chem. Res.* **2001**, *34*, 257–264.
(36) Gao, J.; Bender, C. M.; Murphy, C. J. *Langmuir* **2003**, *19*, 9065–9070.
(37) Jana, N. R.; Gearheart, L.; Murphy, C. J. *J. Phys. Chem. B* **2001**, *105*, 4065–4067.

MA900169J